



HAL
open science

Analysis and modeling of SDS and DPC micelle SAXS data for membrane protein solution structure characterization

Alexandre Pozza, Françoise Bonneté

► **To cite this version:**

Alexandre Pozza, Françoise Bonneté. Analysis and modeling of SDS and DPC micelle SAXS data for membrane protein solution structure characterization. *Data in Brief*, 2023, 47, pp.108915. 10.1016/j.dib.2023.108915 . hal-03955998

HAL Id: hal-03955998

<https://hal.science/hal-03955998>

Submitted on 3 Feb 2023

HAL is a multi-disciplinary open access archive for the deposit and dissemination of scientific research documents, whether they are published or not. The documents may come from teaching and research institutions in France or abroad, or from public or private research centers.

L'archive ouverte pluridisciplinaire **HAL**, est destinée au dépôt et à la diffusion de documents scientifiques de niveau recherche, publiés ou non, émanant des établissements d'enseignement et de recherche français ou étrangers, des laboratoires publics ou privés.



Distributed under a Creative Commons Attribution - NonCommercial 4.0 International License

Article information

Analysis and modeling of SDS and DPC micelle SAXS data for membrane protein solution structure characterization.

Alexandre POZZA & Françoise BONNETÉ*

Affiliations

Université Paris Cité, CNRS, Laboratoire de Biologie Physico-Chimique des Protéines Membranaires (IBPC), F-75005 Paris, France

Corresponding author's email address and Twitter handle

bonnete@ibpc.fr

Keywords

Surfactant micelles, Small Angle X ray Scattering, analytical modeling, Structure, Interactions

Abstract

Herein, we present analysis and analytical modeling of Small Angle X-ray Scattering (SAXS) data on two surfactants forming micelles (i.e., sodium dodecyl sulfate and dodecyl phosphocholine) and used for the study in solution of mTSP0, the translocator membrane protein from *Mus musculus*, as supporting data of the research article published in Biochimie [1].

For both surfactants, concentration series were measured at two Synchrotron SAXS-beamlines. After reduction, buffer subtraction and water calibration of the data, SAXS curves were normalized to surfactant concentration to highlight possible changes in micelle shape or presence of inter-micellar weak interactions. They were then analyzed in terms of radius of gyration (R_G), absolute forward intensity ($I(0)$) to access the surfactant aggregation number (N_a) and pair-distance distribution function ($P(r)$), which gives information on the shape and dimensions of the micelles. Finally, an analytical modeling using SasView - a SAS analysis software package (<https://www.sasview.org/>) - was performed to describe structural features of the two surfactant micelles at a concentration at which no change in the micelle shape nor weak interactions are observed. A core-shell ellipsoidal model was used to fit the SAXS curves, which provided geometrical parameters of the micelles (equatorial and polar radii, shell thickness) and also scattering length

densities (SLD) of both the hydrophobic core and the hydrophilic shell. Hydration of polar heads into the micelle shell could be estimated from micelle volume calculations (V_{core} and V_{shell}). These parameters are particularly useful when modeling SAXS curves of membrane protein-surfactant complexes as described in Combet *et al* [1].

Specifications table

Subject	Physical Chemistry
Specific subject area	Small Angle X-ray Scattering analysis and analytical modeling
Type of data	Graph, table, image
How the data were acquired	<p>Small Angle X-ray Scattering data were collected either at the European Synchrotron Radiation Facility ESRF (Grenoble, France) on the beamline BM29 or at the French Synchrotron SOLEIL (St Aubin, France) on the beamline Swing, both in the framework of BAG (Block Allocation Group) beamtimes.</p> <p>BM29@ESRF is a highly automated SAXS beamline, using the EDNA framework, which allows azimuthal integration, background subtraction and analysis of scattering curves.</p> <p>Data collected on Swing@SOLEIL are reduced using the program Foxtrot.</p> <p>SAXS curves are then analyzed using either the ATSAS package from EMBL (Hamburg) or BioXTAS Raw software.</p>
Data format	Raw data (.dat), Analyzed data (.csv)
Description of data collection	<p>SDS and DPC stock solutions were prepared in buffer-NaCl solutions at room temperature. Concentration series of SDS and DPC in buffer solutions were collected at 20°C. Several images were collected for each concentration and related buffer. Reduced data were averaged when no radiation damage was observed, then the buffer signal was subtracted and the data were finally normalized with surfactant concentration.</p>
Data source location	IBPC, Paris, France

Data accessibility	<p>Raw data and analyzed data linked to graphs are with this article. They are also publicly available in the generalized repository Mendeley data at https://data.mendeley.com/datasets/fjwcpndk3d</p> <p>Repository name: Bonneté, Françoise; Pozza, Alexandre (2022), "SDS and DPC SAXS data", Data identification number: DOI: 10.17632/fjwcpndk3d.1</p>
Related research article	<p>S. Combet, F. Bonneté, S. Finet, A. Pozza, C. Saade, A. Martel, A. Koutsioubas, and J-J. Lacapère, "Effect of amphiphilic environment on the solution structure of mouse TSPO translocator protein", <i>Biochimie</i> (2022), 10.1016/j.biochi.2022.11.014.</p>

Value of the data

- SAXS is a powerful tool to describe surfactant micelle structure and interactions
- The concentration-dependent SAXS data can reveal shape evolution in micelle formation and inter-micellar effects. This kind of information can be useful for researchers to explain surfactant solution properties and its effect on membrane proteins.
- The present SAXS data can be useful for researchers who conduct computational modeling.

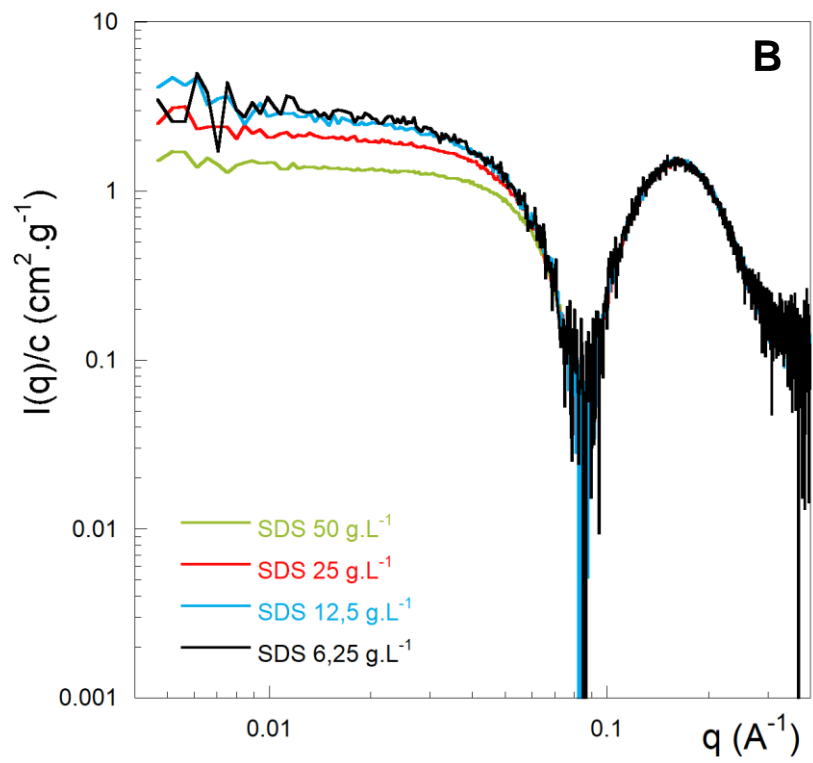
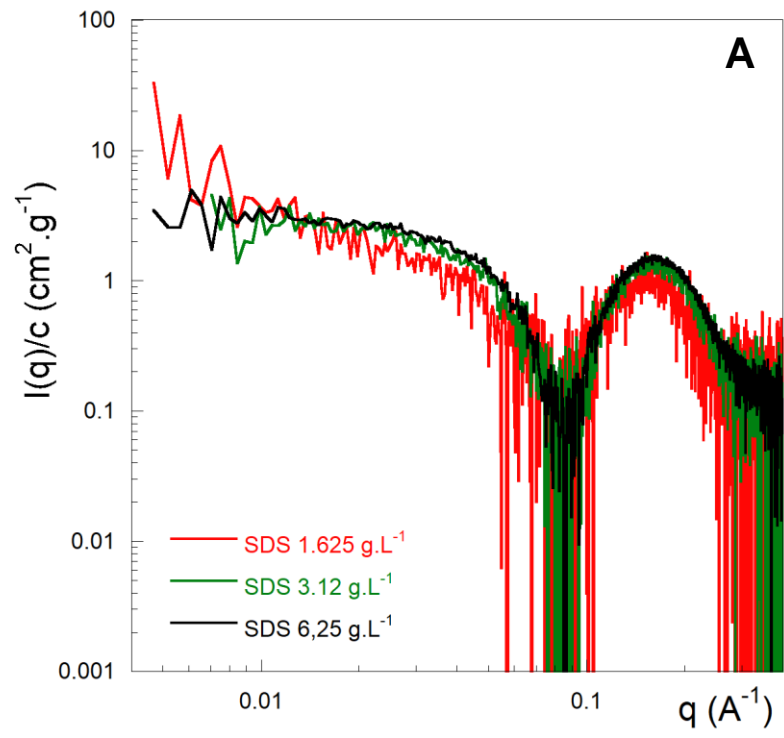
Objective

The data shown in the present article are related to our recent study of mTSPO, a mammalian translocator membrane protein, whose solution structure was compared in two surfactant environments, SDS and DPC [1]. The molecular modeling of the mTSPO-surfactant complex in the two surfactants has been performed by scattering techniques (light, X-ray and neutron scattering). This required a thorough description of the surfactant micelle properties (scattering length densities of polar head and hydrophobic tail) and micelle structural parameters (hydrophobic core dimensions, polar shell thickness) from SAXS curve modeling, all parameters useful to perform modeling of the surfactant belt around mTSPO using the program MemProt [2].

Data description

SAXS experiments were conducted for two surfactants, sodium dodecyl sulfate (SDS) and dodecyl phosphocholine (DPC), as a function of surfactant concentration above their respective CMC (critical micelle concentration), in the same buffer conditions as those used to study the membrane protein-surfactant complexes, mTSPO-SDS and mTSPO-DPC, described in [1]. Characteristic parameters of the two surfactants are presented in Table 1. The SAXS data were collected at two synchrotron beamlines, BM29 at ESRF (Grenoble, France) and Swing at SOLEIL (St Aubin, France). 1D-reduced, buffer-subtracted and water-calibrated SAXS data were normalized for surfactant concentration in $\text{g}\cdot\text{cm}^{-3}$ and $I(q)/c$ was plotted as a function of the scattering vector $q = 4\pi\sin\theta/\lambda$ in \AA^{-1} (Figure 1). For both surfactants, two regimes of concentration dependence can be observed on the scattering curves. At low concentrations, below $6.25 \text{ g}\cdot\text{L}^{-1}$ for SDS and $5 \text{ g}\cdot\text{L}^{-1}$ for DPC, a change in the micelle form factor (*i.e.*, micelle shape) is observed (Figure 1A and 1C), whereas at high concentrations, above $6.25 \text{ g}\cdot\text{L}^{-1}$ for SDS and $5 \text{ g}\cdot\text{L}^{-1}$ for DPC, a concentration-dependent structure factor (*i.e.*, inter-micellar interactions) appears (Figure 1B and 1D). Using the Guinier approximation (Eq. 1) in a q -range such that $q\cdot R_G < 1.3$, we obtain for each concentration both the surfactant aggregation number (N_a) from the absolute forward intensity ($I(0)$) and the radius of gyration (R_G) for SDS and DPC micelles (Figure 2). Indirect Fourier Transform (IFT) using the program GNOM and analytical modeling using the software SasView were performed on the SAXS curve that presented for each surfactant a stable form factor and no structure factor, *i.e.*, $6.25 \text{ g}\cdot\text{L}^{-1}$ for SDS and $5 \text{ g}\cdot\text{L}^{-1}$ for DPC. The pair-distance distribution function ($P(r)$) (Figure 3) and the analytical core-shell model (Figure 4) provide us with characteristic distances of SDS and DPC micelles (*i.e.*, core radius (R_c), maximum dimension (D_{max}), equatorial (R_{eq}) and polar radius (R_{po}), shell thickness (T_{sh})). The fitting parameters obtained from the SasView modeling are listed in the Table 2. Data shown in Figs.1–4 are available in numerical tabular forms (.csv files) in Mendeley repository data. The corresponding subtracted SAXS data in absolute scale (cm^{-1}) are also available as .dat files in (q , $I(q)$, *error*) format.

Figure 1. Concentration-normalized SAXS intensities for the two surfactants are separated between low and high concentrations. (A) SDS micelles below $5 \text{ g}\cdot\text{L}^{-1}$ and (B) above $5 \text{ g}\cdot\text{L}^{-1}$, (C) DPC micelles below $6.25 \text{ g}\cdot\text{L}^{-1}$ and (D) above $6.25 \text{ g}\cdot\text{L}^{-1}$. Concentrations are specified in the figure insert.



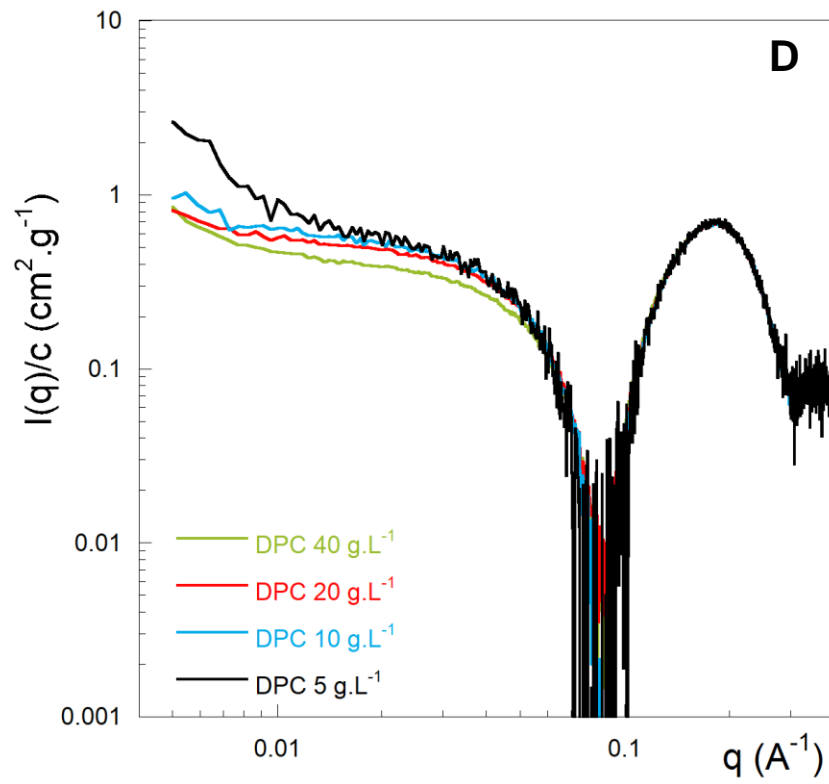
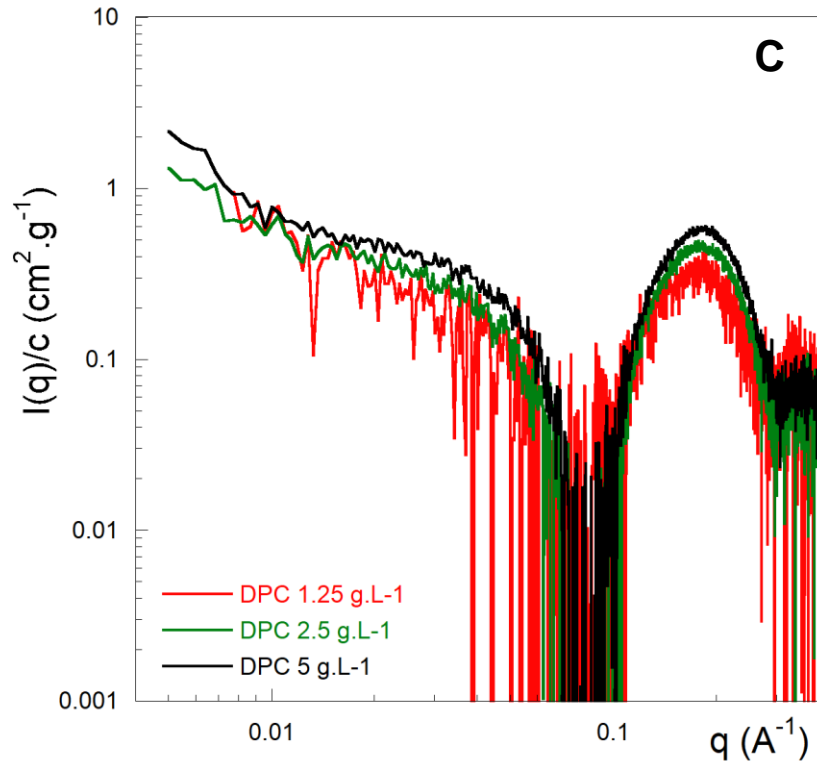


Figure 2: (A) Aggregation number (N_a); (B) radius of gyration (R_G) obtained for SDS (blue dots) and DPC (red dots) micelles as a function of the surfactant concentration.

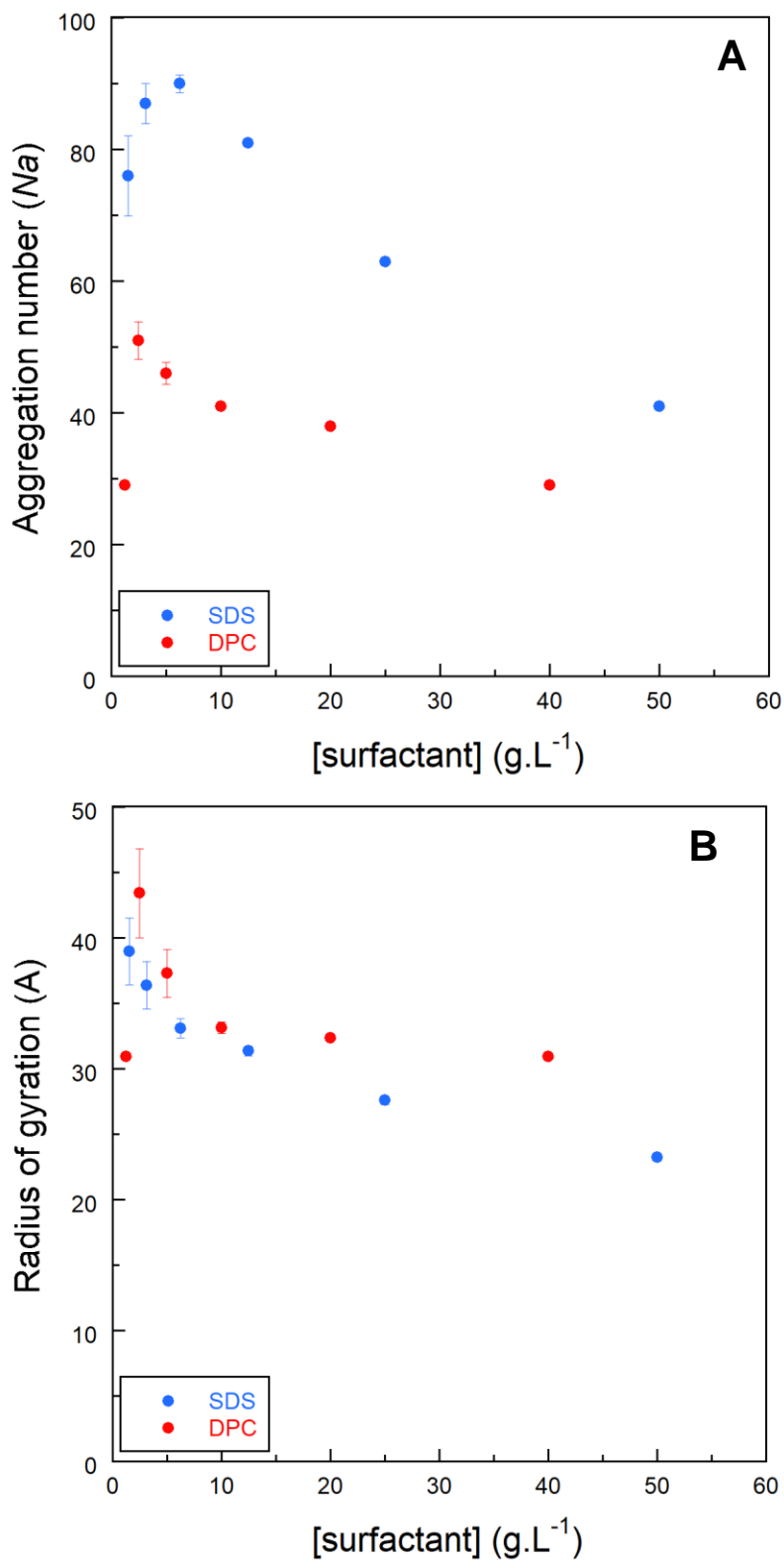


Figure 3: Pair-distance distribution function ($P(r)$) obtained for SDS (blue line) and DPC (red line) micelles at 6.25 and 5 g.L⁻¹, respectively. The solid arrows indicate an estimation of the micelle core radius (R_c) and the maximum dimension of micelles (D_{max}).

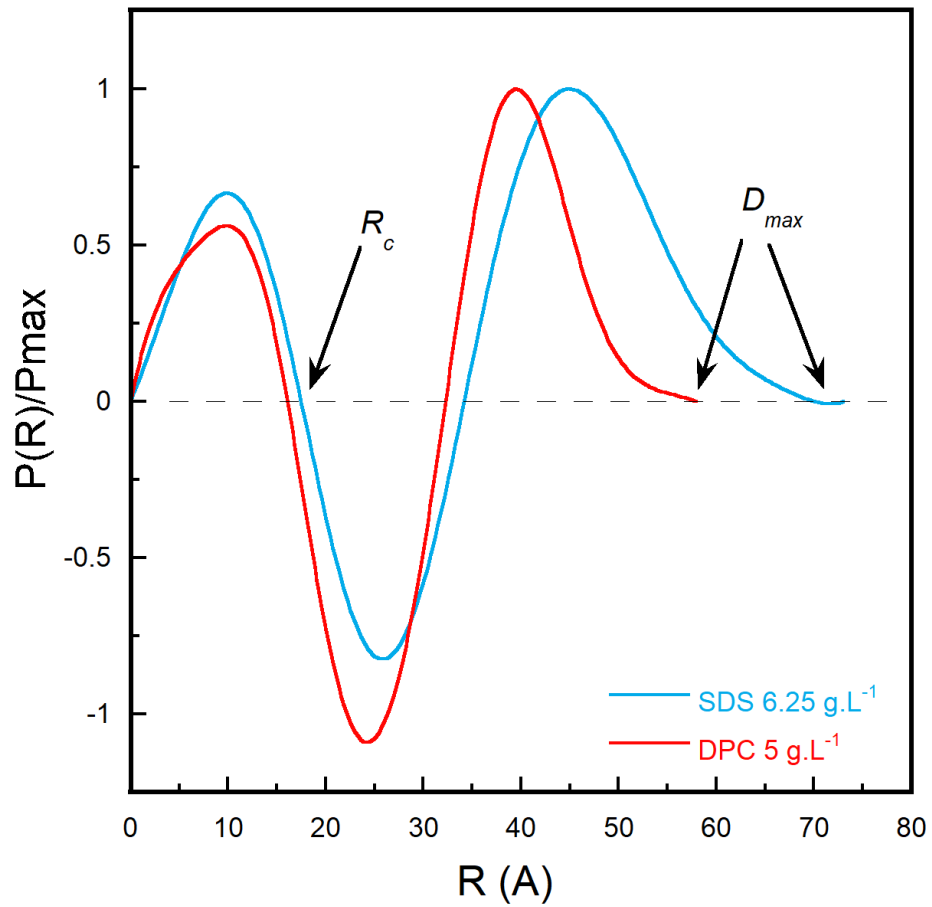


Figure 4: (A) The ellipsoid core-shell analytical model used in the SasView software; (B) Model computation obtained for SDS micelle at 6.25 g.L⁻¹ (blue dots) and DPC micelle at 5 g.L⁻¹ (red dots); (C) Corresponding residuals.

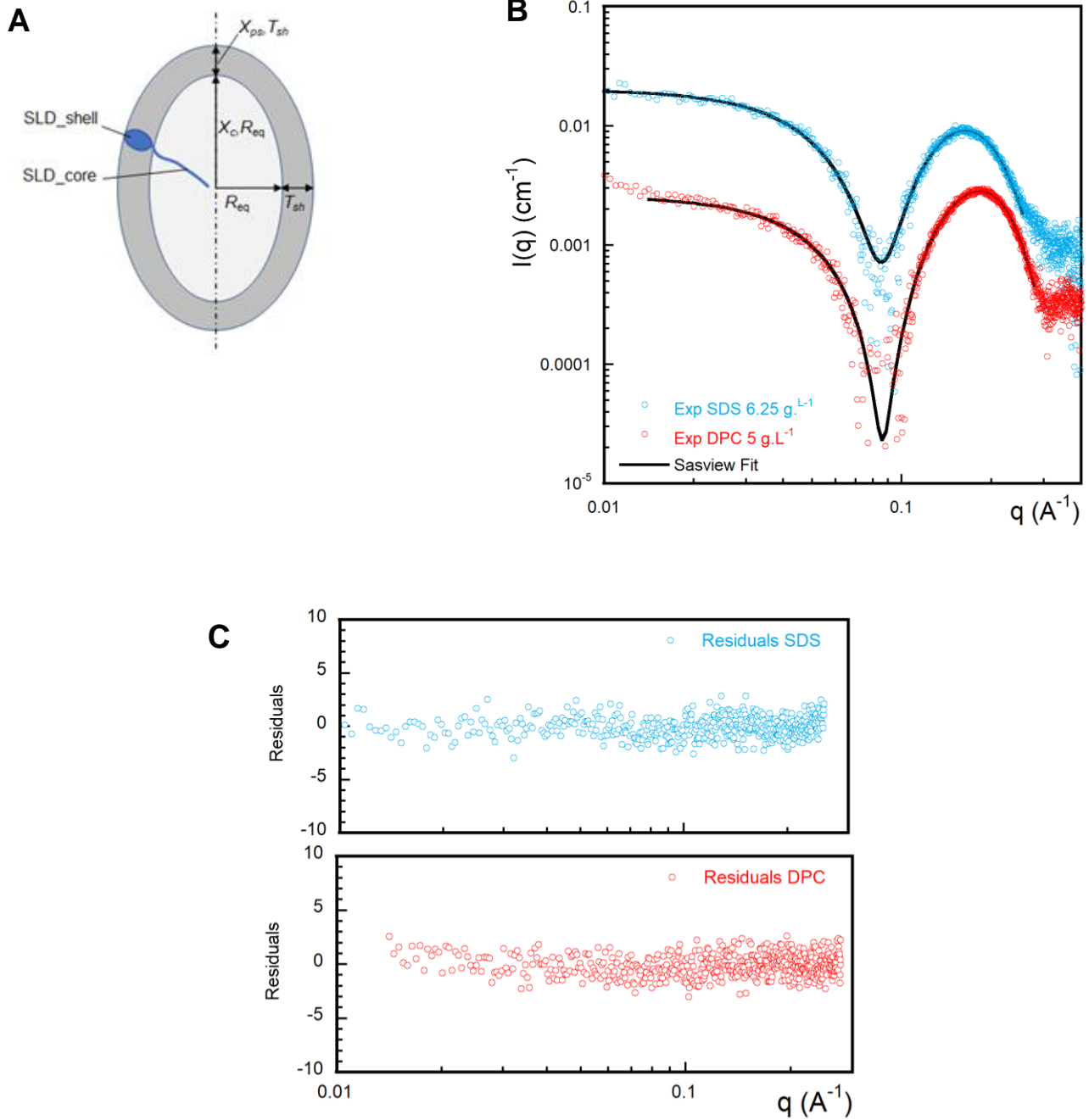


Table 1: Surfactant characteristics

Parameters	Surfactant	SDS	DPC
Chemical formula		$C_{12}H_{25}SO_4Na$	$C_{17}H_{38}NO_4P$
Formula molecular weight ($g \cdot mol^{-1}$) M_{surf}		288.4	351.5
Number of electrons in the head		59	97
Number of electrons in the tail		97	97
CMC ($g \cdot L^{-1}$) in 10 mM NaPhosphate, 150 mM NaCl, pH 7		0.21	-
CMC ($g \cdot L^{-1}$) in 50 mM HEPES, 150 mM NaCl, pH 7		-	0.31
V_p ($cm^3 \cdot g^{-1}$)		0.815 [†]	0.937 [‡]
V_{det} (\AA^3) from V_p		390	547
V_{tail} (\AA^3)*		350.2	350.2
$V_{anhydrous\ head}$ (\AA^3) calculated		39.8	196.8
V_{H_2O} (\AA^3)		30	30

[†] [3] ; [‡] [4] ; * $V_{tail} = 27.4 + 26.9N_c$, with N_c length of hydrocarbon tail [5].

CMC (critical micelle concentration) were measured by fluorescence using ANS as a probe, as described in [6]

Table 2. SasView fitting parameters obtained from SDS and DPC micelle SAXS data.

Parameters	SDS 6.25 mg/mL	DPC 5 mg/mL
Fit optimizer	DREAM	DREAM
Model	Core-shell ellipsoid	Core-shell ellipsoid
q -range (min, max) (\AA^{-1})	0.0084, 0.255	0.0141, 0.278
Chi ² /Npts	0.97	1.09
scale	0.00512	0.0047
background (cm^{-1})	$0.00040 \pm 4.4 \cdot 10^{-5}$	$2.42 \cdot 10^{-7} \pm 8.2 \cdot 10^{-7}$
radius of equatorial core, R_{eq} (\AA)	17.82 ± 0.019	14.61 ± 0.12
x_{core} , X_c	1.75 ± 0.11	1.52 ± 0.014
radius of polar core, $R_{po} = X_c \cdot R_{eq}$ (\AA)	31.185 ± 1.99	22.207 ± 0.38
shell thickness, T_{sh} (\AA)	4.85 ± 0.17	6.83 ± 0.22
x_{polar_shell} , X_{ps} (fixed)	1	1
SLD _{core} ($10^{-6}/\text{\AA}^2$)	7.34 ± 0.12	7.54 ± 0.027
SLD _{shell} ($10^{-6}/\text{\AA}^2$)	13.28 ± 0.16	10.91 ± 0.054
SLD _{solvent} ($10^{-6}/\text{\AA}^2$) (fixed)	9.4	9.4
volume of the core (\AA^3)	41,481	19,855
volume of the shell (\AA^3)	77,574	55,910
N_{a_mod} from model	118	56
N_a from $I(0)$	90	36
N_{H_2O} per head	9	14

Experimental design, materials and methods

Materials

All salt and buffer reagents were purchased from Sigma-Aldrich or Anatrace: sodium dodecyl sulfate (SDS) was obtained from Sigma-Aldrich (CAS number 151-21-3) and dodecyl phosphocholine (DPC) from Anatrace (CAS number 29557-51-5).

Sample preparation

A SDS stock solution was prepared at 50 g.L⁻¹ in 10 mM Phosphate buffer, pH 7, 150 mM NaCl and a DPC stock solution at 40 g.L⁻¹ in 50 mM Hepes buffer, pH 7, 150 mM NaCl. Concentration series were prepared by two-fold successive dilution from 50 to 0.4 g.L⁻¹ for SDS and from 40 to 0.3 g.L⁻¹ for DPC. All salt and buffer solutions were prepared with Milli-Q water at room temperature.

SAXS measurements

These SAXS experiments were performed in the framework of Block Allocation Groups (BAGs), which facilitate access to beamtime on synchrotron beamlines.

Thus, SAXS experiments on SDS micelles were performed in batch mode (automatically pipetted from Eppendorf PCR tube strips) on the BioSAXS beamline BM29 (ESRF, Grenoble, France) [7]. With a wavelength of $\lambda = 0.9919 \text{ \AA}$ and a sample-to-detector distance of 2.849 m, the achievable q -range was 0.00375 to 0.4946 \AA^{-1} . Ten 2D-images of 0.5 s exposure each were collected for each SDS concentration and corresponding buffer. A pipeline driven by EDNA [8] provides automatic data processing (*i.e.* raw data, averaged data and buffer-subtracted data). The subtracted data were put in absolute scale (cm^{-1}) after incident beam calibration using water as standard [9].

SAXS experiments on DPC micelles were performed in batch mode (automatically pipetted from 250 μL Agilent vials) on the BioSAXS beamline SWING at the French synchrotron facility (SOLEIL, St-Aubin, France) [10], using a wavelength of $\lambda = 1.03 \text{ \AA}$ and a sample-to-detector distance of 2 m. The achievable q -range was 0.0045 to 0.546 \AA^{-1} . 40 images of 990 ms each were collected for each DPC concentration and corresponding buffer. The 2D-SAXS patterns were normalized with respect to the transmitted intensity and azimuthally averaged using the Foxtrot program (Java-based graphical application

developed at SOLEIL and available at <http://www.synchrotron-soleil.fr/Recherche/LignesLumiere/SWING>) [11]. For each concentration, 1D-row data were averaged when no radiation damage was observed and buffer-subtracted.

All sample tubes or vials were stored in the sample changer and automatically collected at 20°C.

SAXS analysis

At the CMC of both surfactants, no significant scattering signal was measured. Absolute intensity curves were therefore normalized to surfactant concentration and analyzed by using BioXTAS RAW v2.0.3, an open-source software [12]. Structural parameters were obtained from Guinier analysis [13]. Radius of gyration (R_G) of surfactant micelles was determined from the slope of the linear Guinier approximation (Eq.1), at very small angles, assuming that $q.R_G < 1.3$.

$$\text{Ln } [I(q)/c] = \text{Ln } [I(0)/c] - [q^2 R_G^2 / 3] \quad \text{Eq.1}$$

Molar masses (M_{Mic}) and aggregation numbers (N_a) of surfactant micelles were calculated from the absolute forward intensity $I(0)$.

$$I(0) (\text{in } \text{cm}^{-1}) = c_{\text{Mic}} M_{\text{Mic}} [r_0 \cdot V_p \cdot (\rho_{\text{surf}} - \rho^0)]^2 / \aleph_{av} \quad \text{Eq.2}$$

$$N_a = M_{\text{Mic}} / M_{\text{surf}} \quad \text{Eq.3}$$

with \aleph_{av} the Avogadro's number, r_0 the classical electron radius ($r_0 = 0.28179 \text{E}^{-12} \text{ cm} \cdot \text{e}^{-1}$), V_p the surfactant partial specific volume ($\text{cm}^3 \cdot \text{g}^{-1}$), c_{Mic} the surfactant concentration in micelle form $\approx c_{\text{surf}}$ the total surfactant concentration ($\text{g} \cdot \text{cm}^{-3}$), M_{Mic} the surfactant micelle molar mass ($\text{g} \cdot \text{Mol}^{-1}$), M_{surf} the surfactant monomer molar mass ($\text{g} \cdot \text{Mol}^{-1}$), ρ_{surf} and ρ^0 the electron densities of the surfactant and buffer ($\text{e} \cdot \text{cm}^{-3}$), respectively.

The pair-distance distribution function ($P(r)$) was determined by Inverse Fourier Transformation (IFT) of the scattering intensity using the program GNOM [14] from the ATSAS package (<https://www.embl-hamburg.de/biosaxs/gnom.html>) [15]. The maximum particle dimensions D_{max} was found when $P(r)$ falls to zero ($D_{\text{max}} \sim 75 \text{ \AA}$ for SDS and $\sim 57 \text{ \AA}$ for DPC). An estimation of the micelle core diameter can be obtained from the scattering intensity second maximum [16] ($q \sim 0.16 \text{ \AA}^{-1}$ for SDS and 0.18 \AA^{-1} for DPC) correlated with the micelle core radius obtained from the inflection point on the ($P(r)$) [17].

Finally, the absolute SAXS intensities of SDS at 6.25 g.L⁻¹ and DPC at 5 g.L⁻¹ were fitted (Fig. 4B) using the program SasView 5.0.4 (<https://www.sasview.org/>) that allows to describe mathematically a geometrical model of the surfactant assemblies. Here, a two-axial core-shell ellipsoid was chosen as model of surfactant micelles with parameters described in Fig. 4A and listed in Table 2. From the equatorial and polar core radii (R_{eq} , R_{po}) and the shell thickness (T_{sh}), the volumes of the hydrophobic core (V_{core}) and the hydrophilic shell (V_{shell}) were calculated and the model-based aggregation number (N_{a_mod}) of the surfactant micelles and the number of water molecules per surfactant head (N_{H_2O}) deduced, by using the following formulas:

$$V_{core} = (4\pi/3).R_{eq}^2.R_{po}$$

$$V_{shell} = (4\pi/3).(R_{eq}+T_{sh})^2.(R_{po}+T_{sh}) - (4\pi/3).R_{eq}^2.R_{po}$$

$$N_{a_mod} = V_{core} / V_{tail}$$

$$N_{H_2O} = ((V_{shell} / N_a) - V_{head}) / V_{H_2O}$$

From the ellipsoid core-shell model, a maximum dimension can be calculated as equal to $2.(R_{po} + T_{sh})$.

Ethics statements

The authors have read and ensure that their work meets the ethical requirements for publication in Data in Brief. Our study does not involve studies in humans and animals.

CRedit author statement

Francoise Bonneté: Conceptualization, Formal analysis, Writing–review & editing;

Alexandre Pozza: Resources, Investigation

Acknowledgments

We gratefully acknowledge ESRF and SOLEIL, large-scale facilities for beamtimes on BM29 and SWING beamlines, respectively, and we thank Dr Petra Pernot (BM29) and Dr Aurélien Thureau (SWING) for their assistance during experiments.

This work benefited from the use of the SasView application, originally developed under NSF award DMR-0520547. SasView contains code developed with funding from the European Union’s Horizon 2020 research and innovation program under the SINE2020 project, grant agreement No 654000.

This research did not receive any specific grant from funding agencies in the public, commercial, or not-for-profit sectors.

Declaration of Interest

The authors declare that they have no known competing financial interests or personal relationships that could have appeared to influence the work reported in this paper.

References

1. Combet, S., Bonneté, F., Finet, S., Pozza, A., Saade, C., Martel, A., Koutsioubas, A., and Lacapère, J.-J., (2022). *Effect of amphiphilic environment on the solution structure of mouse TSPO translocator protein* Biochimie, <https://doi.org/10.1016/j.biochi.2022.11.014>
2. Perez, J. and Koutsioubas, A., (2015). *Memprot: a program to model the detergent corona around a membrane protein based on SEC-SAXS data* Acta Crystallographica D, <https://doi.org/10.1107/s1399004714016678>
3. Tanford, C., Nozaki, Y., Reynolds, J.A., and Makino, S., (1974). *Molecular characterization of proteins in detergent solutions* Biochemistry, <https://doi.org/10.1021/bi00708a021>
4. Le Maire, M., Champeil, P., and Moller, J.V., (2000). *Interaction of membrane proteins and lipids with solubilizing detergents* Biochim Biophys Acta, [https://doi.org/10.1016/S0304-4157\(00\)00010-1](https://doi.org/10.1016/S0304-4157(00)00010-1)
5. Tanford, C., (1980). *The hydrophobic effect: Formation of micelles and biological membranes*. Vol. 18, New York: John Wiley & Sons, Inc. 687.
6. De Vendittis, E., Palumbo, G., Parlato, G., and Bocchini, V., (1981). *A fluorimetric method for the estimation of the critical micelle concentration of surfactants* Anal Biochem, 10.1016/0003-2697(81)90006-3
7. Pernot, P., Theveneau, P., Giraud, T., Nogueira Fernandes, R., Nurizzo, D., Spruce, D., Surr, J., McSweeney, S., Round, A., Felisaz, F., Foedinger, L., Gobbo, A., Huet, J., Villard, C., and Cipriani, F., (2010). *New beamline dedicated to solution scattering from biological macromolecules at the ESRF* Journal of Physics: Conference Series, <http://stacks.iop.org/1742-6596/247/i=1/a=012009>
8. Incardona, M.F., Bourenkov, G.P., Levik, K., Pieritz, R.A., Popov, A.N., and Svensson, O., (2009). *EDNA: a framework for plugin-based applications applied to X-ray experiment online data analysis* J Synchrotron Radiat, <https://doi.org/10.1107/s0909049509036681>
9. Orthaber, D., Bergmann, A., and Glatter, O., (2000). *SAXS experiments on absolute scale with Kratky systems using water as a secondary standard* Journal of Applied Crystallography, <https://doi.org/10.1107/S0021889899015216>
10. David, G. and Perez, J., (2009). *Combined sampler robot and high-performance liquid chromatography: a fully automated system for biological small-angle X-ray scattering experiments at the Synchrotron SOLEIL SWING beamline* Journal of Applied Crystallography, <https://doi.org/10.1107/S0021889809029288>
11. Girardot, R., Viguier, G., Pérez, J., and Ounsy, M. (2015) *FOXTROT: A JAVA-Based Application to Reduce and Analyse SAXS and WAXS Piles of 2D Data at Synchrotron Soleil*. in *canSAS-VIII*. Tokai, Japan.
12. Hopkins, J.B., Gillilan, R.E., and Skou, S., (2017). *BioXTAS RAW: improvements to a free open-source program for small-angle X-ray scattering data reduction and analysis* Journal of Applied Crystallography, <https://doi.org/10.1107/S1600576717011438>
13. Guinier, A. and Fournet, G., (1955). *Small angle scattering of X-rays* New York: Ed. Wiley.

14. Svergun, D.I., (1992). *Determination of the Regularization Parameter in Indirect-Transform Methods Using Perceptual Criteria* Journal of Applied Crystallography, <https://doi.org/10.1107/S0021889892001663>
15. Franke, D., Petoukhov, M.V., Konarev, P.V., Panjkovich, A., Tuukkanen, A., Mertens, H.D.T., Kikhney, A.G., Hajizadeh, N.R., Franklin, J.M., Jeffries, C.M., and Svergun, D.I., (2017). *ATSAS 2.8: a comprehensive data analysis suite for small-angle scattering from macromolecular solutions* J Appl Cryst., <https://doi.org/10.1107/S1600576717007786>
16. Oliver, R.C., Lipfert, J., Fox, D.A., Lo, R.H., Doniach, S., and Columbus, L., (2013). *Dependence of Micelle Size and Shape on Detergent Alkyl Chain Length and Head Group* PLoS ONE, <https://doi.org/10.1371/journal.pone.0062488>
17. Gawali, S.L., Zhang, M., Kumar, S., Ray, D., Basu, M., Aswal, V.K., Danino, D., and Hassan, P.A., (2019). *Discerning the Structure Factor of Charged Micelles in Water and Supercooled Solvent by Contrast Variation X-ray Scattering* Langmuir, <https://doi.org/10.1021/acs.langmuir.9b00912>